

Coherent detection schemes for subcarrier wave continuous variable quantum key distribution system

E Samsonov¹, R Goncharov¹, M Fadeev¹, A Zinoviev¹,
D Kirichenko¹

¹ ITMO University, Kronverkskiy, 49, St.Petersburg, 197101, Russia

E-mail: eosamsonov@itmo.ru

Abstract. In this paper, we demonstrate different approaches to coherent detection implementation in subcarrier wave quantum communication schemes. In order to extract information from quadrature phase-coded multimode signals, we demonstrate models of homodyne, double homodyne, and heterodyne detection, actively using the properties of such signals to implement. For greater clarity, all mathematical calculations are given in terms of wave optics. The feasibility of the proposed schemes is supported by experiments.

Keywords: coherent detection, subcarrier wave, multimode states, quantum communication

1. Introduction

Since 1896, when the "beat receptor", the first heterodyne detector, as we know it now, was invented by Nicola Tesla [1], various forms of coherent detection methods, including homodyne and heterodyne detection, found wide range of applications. Started with radio communications [2], coherent detection methods being expanded to the optical domain [3]. Nowadays there is a broad range of examples of optical coherent detection usage in lots of different fields including communication [4, 5, 6, 7, 8] and quantum optics [9, 10, 11]. One of the promising technology at the boundary between communications and quantum optics is quantum key distribution (QKD), which, in combination with coherent detection, leads to a separate branch known as continuous variable (CV) QKD [12, 13, 14, 15, 16, 17, 18]. CV-QKD systems relies on methods of coherent detection for gaining information encoded in the quadratures of the electromagnetic field. In other words, single-photon detection can be replaced by conventional optical communication methods in particular homodyne or heterodyne detection.

Due to the active development of novel QKD systems using non-standard states of light there is a necessity to upgrade existing detection schemes. The subcarrier wave (SCW) QKD [19, 20, 21, 22, 23, 24, 25, 26] is striking example of such a system. A defining property of subcarrier wave QKD is the method for quantum state encoding. In it, a strong monochromatic wave emitted by a laser is modulated in an electro-optical phase modulator to produce weak sidebands, whose phase with respect to the strong (carrier) wave encodes quantum information (for more details, see [21]). Like in any other discrete variable QKD systems, in SCW QKD the weak radiation component is detected by a single photon counter, and the measured observable has a discrete spectrum.

In this paper we present three new coherent detection schemes with phase estimation to demodulate quadrature phase-coded multimode signals. This type of signals is used to encode quantum information in SCW QKD systems. The main advantage of proposed schemes is using the carrier wave (an essential part of SCW methodology) as a local oscillator. In practice, it solves the well-known problem of transmitting the local oscillator through the quantum channel (or its generation on receivers side). This is a novel approach that has not been discussed in previous works dedicated to studying multimode CV QKD [27, 28, 29]. Here we compose a mathematical models of the proposed detection schemes and experimentally demonstrate the possibility to implement coherent detection using the carrier wave as a local oscillator.

2. Phase-coded multimode signals generation

First we describe phase-coded multimode signals generation which is essential part of SCW QKD system. Since we implement proof-of-principle experiment with classical light, we employ the known classical model for electro-optical phase modulation [30]. The detailed description of electro-optic modulation process for quantum states can be found in [31, 32, 33]. As it shown in Fig. 1 monochromatic light at frequency ω and with amplitude given by A_0 is modulated in the traveling wave electro-optical phase modulator with the microwave field with frequency Ω and phase φ_a [34]. The phase-modulated optical field $E(t)$ can be expressed in terms of JacobiAnger expansion as follows

$$E(t) = E_0 e^{i\omega t} e^{im_a \cos(\Omega t + \varphi_a)} = E_0 e^{i\omega t} \sum_{k=-\infty}^{\infty} i^k J_k(m_a) e^{ik(\Omega t + \varphi_a)}, \quad (1)$$

where $J_k(m_a)$ is the k -order Bessel function of the first kind, argument of the Bessel function m_a is modulation index, which is chosen to be small. As a result, sidebands are formed at frequencies $\omega_k = \omega + k\Omega$ with integer k . where integer k runs between the limits: $-\infty \leq k \leq \infty$. The typical power spectrum at the modulator output in SCW QKD are shown in Fig. 1.

The light beam thus obtained at the output of phase modulator contains the reference carrier ω_0 ($k = 0$) and the sidebands ω_k ($k \neq 0$). The relative phase and

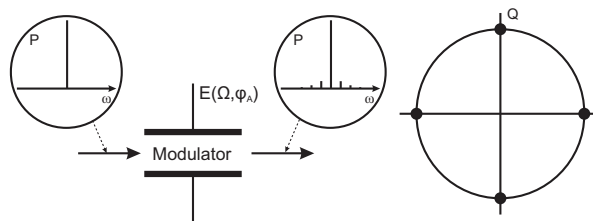


Figure 1: Modulated light emerging after the electro-optical phase modulator and 4-PSK constellation diagram

amplitude between reference and all the sidebands can be controlled by the inner microwave field via controlling the phase φ_a and modulation index m_a , respectively. Hence one can encode information into sidebands of phase-modulated light applying different forms of quadrature amplitude modulation [20, 21, 35, 36, 37]. In this paper for the simplicity we consider quadrature phase-shift keying, which is extensively used in CV-QKD with discrete modulation [18, 38, 39]. Here we prepare phase-coded multimode signals by selecting the phase of the microwave field from the finite set of $\varphi_a \in \{0, \pi/2, \pi, 3\pi/2\}$. An example of a modulated signal constellation diagram can be seen in Fig. 1.

3. Coherent detection with quadrature component selection

Here we consider SCW QKD system with coherent in a simplified classical way. We formally leave Alice's block the same as in initial system [21] but completely change the detection scheme. Fig. 2 describes the operation of proposed coherent detection scheme in detail.

By definition, homodyne detection is characterized by interference of a weak signal with a powerful local oscillator on a 50/50 beam splitter. After interference, the mean number of photons at the detectors n_1 and n_2 depends on phase difference $\Delta\phi = \phi_a - \phi_b$. Then, the difference in photo-electrons n_e can be determined by signal subtraction through the measuring of current. Coherent detection scheme employed in this work is similar to homodyne detection. Homodyning in continuous variable SCW is carried out directly in the phase modulator in the Bob module (instead of a 50/50 beam splitter) for each sideband independently. After the second modulation interference is observed at frequencies $\omega_k = \omega + k\Omega$ if equal modulator's microwave field frequencies Ω are used by Alice and Bob. Resulting power depends on phase difference $\Delta\varphi = \varphi_a - \varphi_b$. In case of constructive (Fig. 3a) or destructive (Fig. 3b) interference, subcarriers wave power becomes either more or less than the carrier wave power, respectively. A narrow spectral filter then separates the carrier from the sidebands. Finally, two outputs (carrier and all the sidebands) are detected by two different photodiodes, and their photo currents are subtracted. Thus, one can extract information encoded in the the oscillating signal phase. Similar to traditional homodyne detection in QKD, Bob measures only one quadrature component at a time by selecting the phase of the microwave field from the

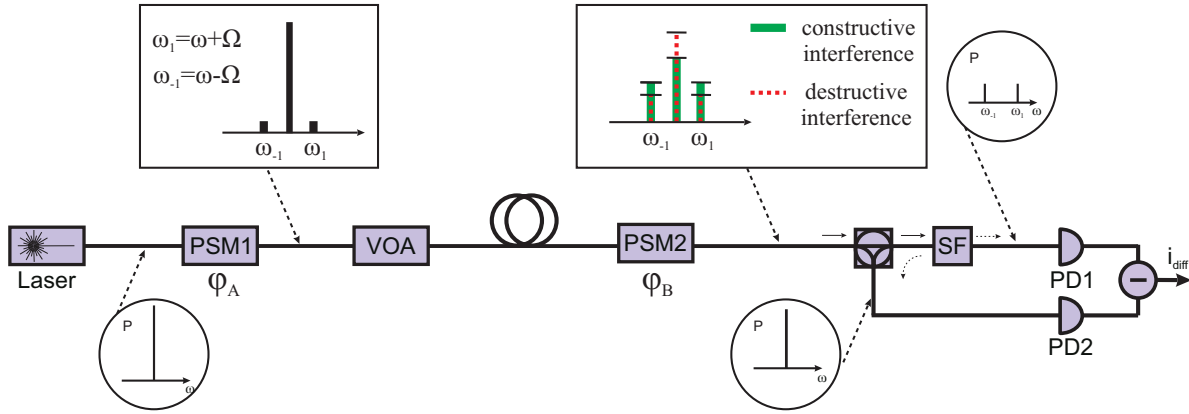


Figure 2: Principal scheme of SCW CV-QKD setup. PSM is an electro-optical phase modulator; VOA is a variable optical attenuator; SF is a spectral filter that cuts off the carrier; PD is a photodiode. Diagrams in circles show the absolute value of signal spectrum taking into account only the first-order subcarriers. Diagrams in squares illustrate the absolute value of signal spectrum and comparison of spectra for various phase shifts; different coherent states are shown on phase plane.

set of $\varphi_b \in \{0, \pi/2, \}$.

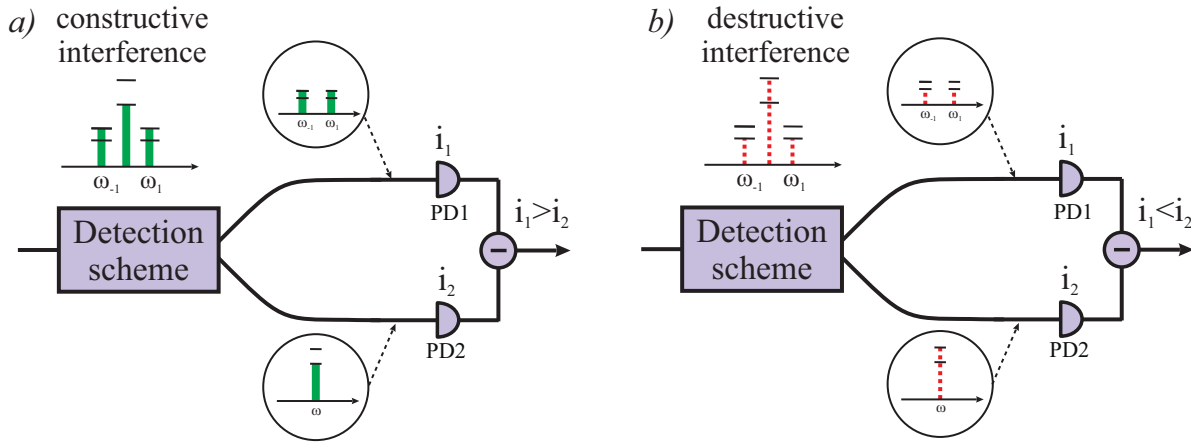


Figure 3: SCW coherent detection scheme operation. The charts show energy distribution between the carrier and the subcarriers in case of constructive (a) and destructive (b) interference. Subcarrier signal power becomes higher or lower than the carrier power, respectively. Horizontal dashes added for illustrative purposes.

3.1. Detection model

The mathematical model presented in this subsection describes the classic case as the most understandable. A similar model in terms of quantum mechanics, which is more justified for the description of QKD systems, is presented in [26].

The traveling wave phase modulator on the Bob's side has the same modulation frequency Ω as in the Alice's one, but a different phase φ_b and modulation index m_b . The resulting double-modulated optical field $E'(t)$ can be expressed as

$$E'(t) = E_0 e^{i\omega t} e^{im_a \cos(\Omega t + \varphi_a)} e^{im_b \cos(\Omega t + \varphi_b)}, \quad (2)$$

which can be rewritten as earlier

$$E'(t) = E_0 e^{i\omega t} \sum_{k=-\infty}^{\infty} i^k J_k(m_1) e^{ik\Psi} \sum_{n=-\infty}^{\infty} J_n(m_2) e^{in\Psi}, \quad (3)$$

where $m_1 = (m_a + m_b) \cos(\Delta\varphi/2)$, $m_2 = (m_b - m_a) \sin(\Delta\varphi/2)$ and $\Psi = \Omega t + (\varphi_a + \varphi_b)/2$. Spectral filtering in Bobs module aims at separating the carrier wave from the sidebands. Here we neglect the losses and imperfection of the spectral filter for simplicity. Fields at the separate arms of the detector are

$$E_1(t) = E_0 e^{i\omega t} \sum_{\tau=-\infty}^{\infty} J_{\tau}(m_1) J_{\tau}(m_2) e^{i\tau\pi/2}, \quad (4)$$

$$E_2(t) = E_0 e^{i\omega t} \left(\sum_{k=-\infty}^{\infty} i^k J_k(m_1) e^{ik\Psi} \sum_{n=-\infty}^{\infty} J_n(m_2) e^{in\Psi} - \sum_{\tau=-\infty}^{\infty} J_{\tau}(m_1) J_{\tau}(m_2) e^{i\tau\pi/2} \right). \quad (5)$$

The output voltage which is proportional to the difference between the photo currents of the two photodiodes i_{diff} in the absence of noise is then derived as

$$V = R(\lambda) G (|E_1(t)|^2 - |E_2(t)|^2), \quad (6)$$

where G is the electronic gain of balanced detector and $R(\lambda)$ is the responsivity of photodiodes. Here we assume that the detectors are insensitive to the optical and differential radio frequencies. The dependence of output voltage V on the phase shift φ_a for the scheme proposed is illustrated in the Fig. 4. One obtains the in-phase component I and the quadrature component Q by selecting the phase $\varphi_b = 0$ and $\varphi_b = \pi/2$ respectively. In order to show equivalence, we have modeled a classical homodyne scheme in which the carrier wave power interfere with the power of all subcarriers on a 50/50 beam splitter [3]. As one can see from the Fig. 4 the output signals from the scheme proposed and from the classical homodyne scheme are overlapping well.

For calculations we use the experimental parameters from the system used in [21]. A 1550 nm 10 μ W fiber-coupled laser directed into the LiNbO₃ electro-optical phase modulator with electrical signal frequency $\Omega = 4.8$ GHz and the modulation index $m_1 = 0.09$. The carrier wave power after the modulation is $P_c = 9.96$ μ W and the power of all subcarriers is $P_s = 40.00$ nW. The modulation index m_2 is adjusted so that the amplitude ratio between the carrier and all the subcarrier waves is unity. After the second modulation the spectral components are then transmitted through the circulator to a fiber Bragg grating spectral filter. The two output ports of the circulator are coupled

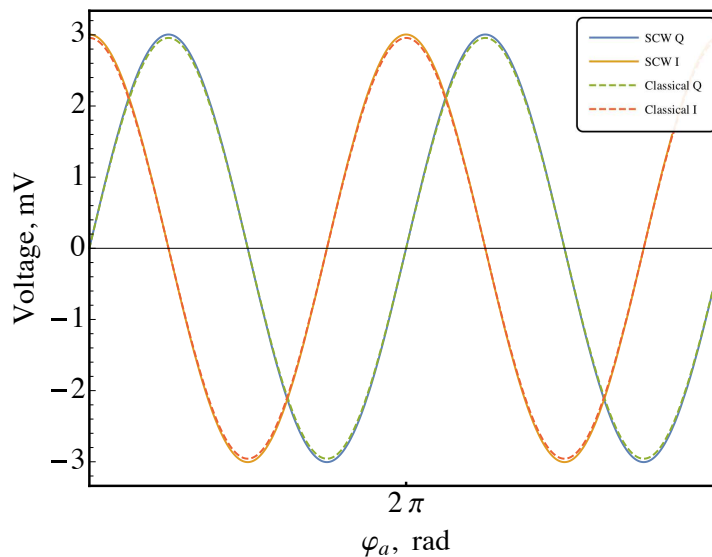


Figure 4: The in-phase and the quadrature components of the output signals from the scheme proposed and from the classical homodyne scheme. One can notice the equivalence of both schemes.

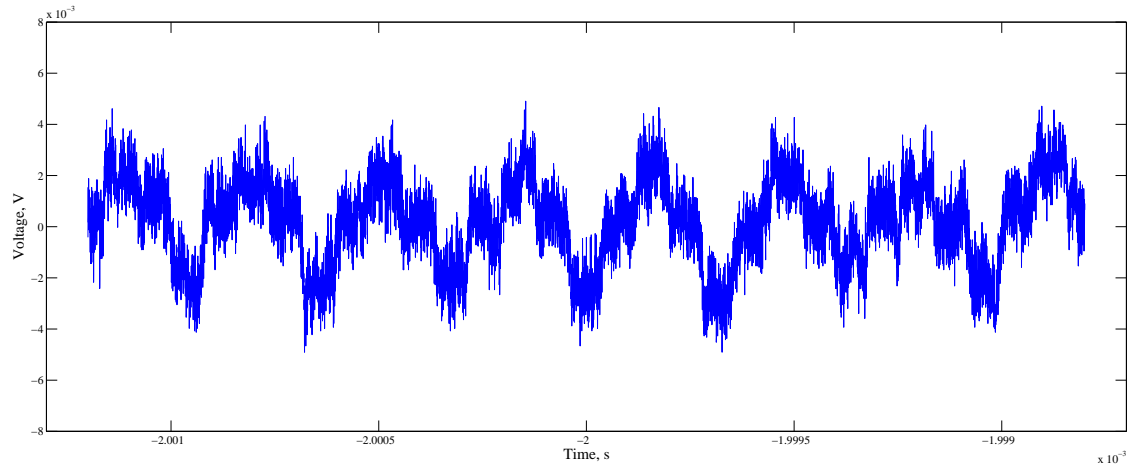
to the input ports of a self-developed balanced detector (measurement bandwidth 100 MHz, $G = 4 \cdot 10^3$, $R = 0.6$).

Using the setup shown in Fig. 2 we implement the proof-of-principle experiment. The Fig. 5 demonstrate the dependence of the output voltage on the relative phase shift $\Delta\varphi$, here the phase φ_b is set to 0 and φ_b alters between finite set of states $\{0, \pi/2, \pi, 3\pi/2\}$. Thus, the coherent detection scheme proposed in this paper is able to estimate the phase of the quadrature phase-coded multimode signals from the electro-optical phase modulator.

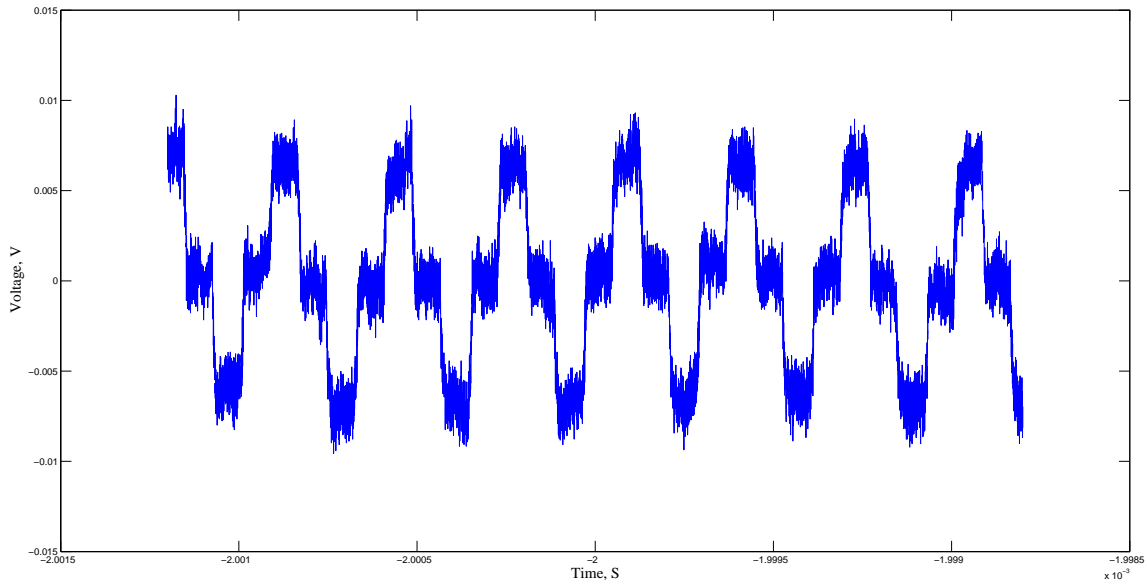
4. Simultaneous selection of both quadrature component

It is important to note that there is a possibility to construct a phase-diversity coherent detection scheme based on proposed coherent detection scheme. The phase-diversity coherent receiver is similar to 90° optical hybrid and allows us to select both quadrature component simultaneously. The principal scheme of SCW CV-QKD setup with phase-diversity coherent receiver is shown in the Fig. 6. Here we use an Y beam splitter and two coherent detection scheme with electro-optical phase modulators whose phase is shifted by 90° in relation to each other.

Using the proposed detection scheme from Fig. 6, we can obtain two outputs $E_{1I}(t)$, $E_{2I}(t)$ from the top arm of the detector and two outputs $E_{1Q}(t)$, $E_{2Q}(t)$ from the bottom arm with the phase $\varphi_b = 0$ and $\varphi_b = \pi/2$ respectively. Then the output differential currents after the balanced detectors are converted to the voltages $V_{I,Q}$. Thus using two balanced detectors one can produce a simultaneous IQ measurements. In Fig. 7 is shown an example of a 4-PSK constellation diagram recovered from the phase-modulated



(a)



(b)

Figure 5: Dependence of the proposed coherent detection scheme output voltage on the time. The extreme points correspond to the constructive and destructive interference. $P_c = 9.96 \mu\text{W}$, $P_s = 40.00 \text{ nW}$ for (a) and $P_c = 9.5 \mu\text{W}$, $P_s = 500.00 \text{ nW}$ for (b).

optical signal. This approach introduces an additional 3 dB loss at the detection stage and in terms of quantum cryptography requires a separate consideration.

5. Heterodyne detection

Another well-known way to restore the full information on the optical complex amplitude is heterodyne detection [3, 6, 40, 41, 42, 43]. Despite that the phase-diversity is more

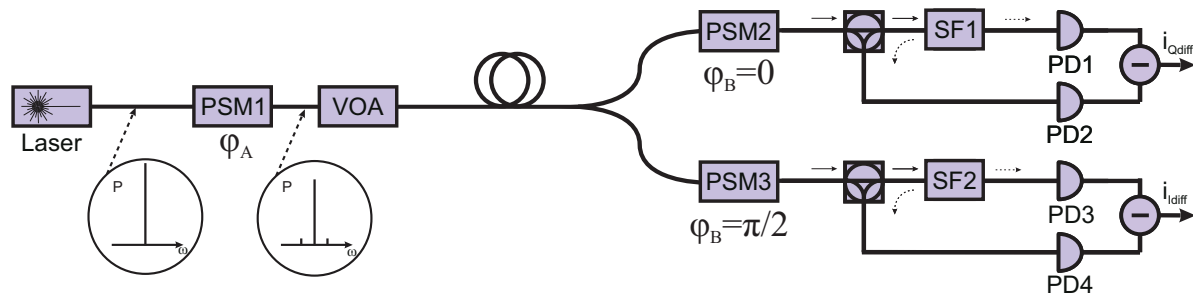


Figure 6: Principal scheme of SCW CV-QKD setup with phase-diversity coherent receiver.

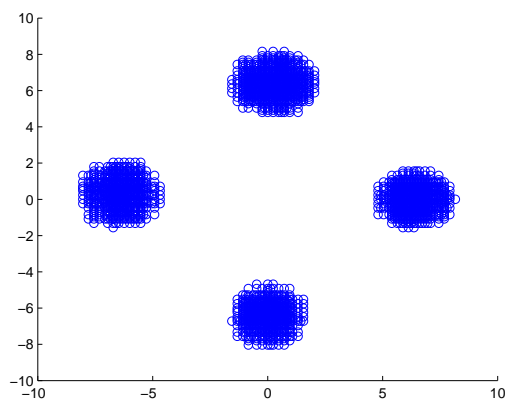


Figure 7: 4-PSK constellation diagram recovered from the phase-modulated optical signal, $P_c = 9.5 \mu\text{W}$, $P_s = 500.00 \text{ nW}$.

advantageous than the heterodyne it is still attractive to implement the heterodyne detection scheme for quadrature phase-coded multimode signals. The scheme that we propose demonstrate versatility of the SCW method and moreover it promise significant simplification of implementation. The Fig. 8 describes the operation of proposed coherent detection scheme.

As in the scheme in the Fig. 2 we leave the Alice's block the same as in the initial system [21, 22] but change the detection scheme. Here we mix the different sidebands with the carrier using spectral filtering to down-convert the signal, including the amplitude and the phase information, to the intermediate frequency. Then we obtain from Eq.(1) the fields at the separate arms:

$$E_1(t) = E_0 e^{i\omega t} \left(\sum_{k=1}^{\infty} i^k J_k(m_a) e^{ik(\Omega t + \varphi_a)} + \sqrt{0.5} J_0(m_a) \right), \quad (7)$$

$$E_2(t) = E_0 e^{i\omega t} \left(\sum_{k=-\infty}^{-1} i^k J_k(m_a) e^{ik(\Omega t + \varphi_a)} + \sqrt{0.5} J_0(m_a) \right), \quad (8)$$

In order to obtain analytical expression for the extracted signal we take into account only the most significant first order subcarriers. Using also the Bessel functions property

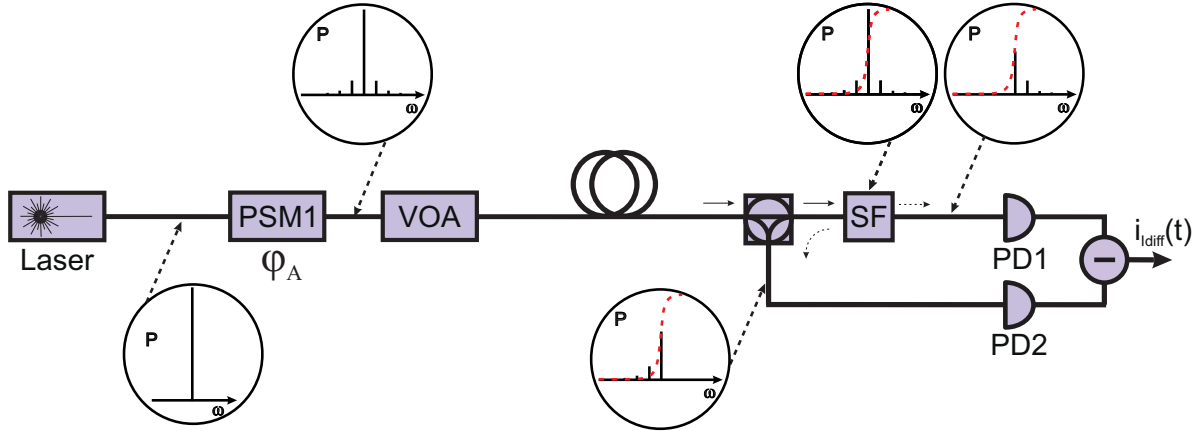


Figure 8: Principal scheme of SCW CV-QKD setup with homodyne detection. Diagrams in the circles illustrate an example of power spectrum.

of $J_{-\alpha}(x) = (-1)^\alpha J_\alpha(x)$ we can write

$$E_1(t) \approx E_0(iJ_1(m_a)e^{i(\omega_- t - \varphi_a)} + \sqrt{0.5}J_0(m_a)e^{i(\omega t)}), \quad (9)$$

$$E_2(t) \approx E_0(iJ_1(m_a)e^{-i(\omega_+ t - \varphi_a)} + \sqrt{0.5}J_0(m_a)e^{i(\omega t)}), \quad (10)$$

where $\omega_- = \omega - \Omega$, $\omega_+ = \omega + \Omega$. The output voltage in the absence of noise can be derived as

$$V(t) = R(\lambda)G(|E_1(t)|^2 - |E_2(t)|^2) = R(\lambda)G2\sqrt{2}E_0^2J_0(m_a)J_1(m_a)\sin(\Omega t + \varphi_a). \quad (11)$$

We can rewrite the complex amplitude in Eq.(11) as

$$V(t) = R(\lambda)G2\sqrt{2}E_0^2J_0(m_a)J_1(m_a)e^{i\varphi_a}, \quad (12)$$

which is completely analogous to the classical heterodyning. Here we assume that the detectors are sensitive to the radio frequency Ω . In the Fig. 9a is the dependence of output voltage on the time for the scheme proposed and for the classical heterodyne in which the carrier wave amplitude at the frequency ω mix with the amplitude of all subcarriers at the frequency Ω on a 50/50 beam splitter. In the Fig. 9b is the dependence of output voltage on the time for the scheme proposed taking into consideration all the subcarriers according to Eq.(7, 8).

Demodulation of the received signal can be carried out by standard telecommunication methods using a quadrature synchronous demodulator [44, 45, 46, 47]. The demodulator setup allows one to observe the in-phase (initial) and quadrature (shifted by $\pi/2$ using a voltage generator) signal components simultaneously on the analyzer and thus obtain information about the selected phase selected by Alice. Thus, quantum information can be extracted without the additional procedure of selecting the quadrature to measure on Bob's side.

The main disadvantage of the proposed heterodyne detector for SCW-QKD system is the necessity to deal with a high intermediate frequency ($\Omega = 4.8$ GHz), contraction

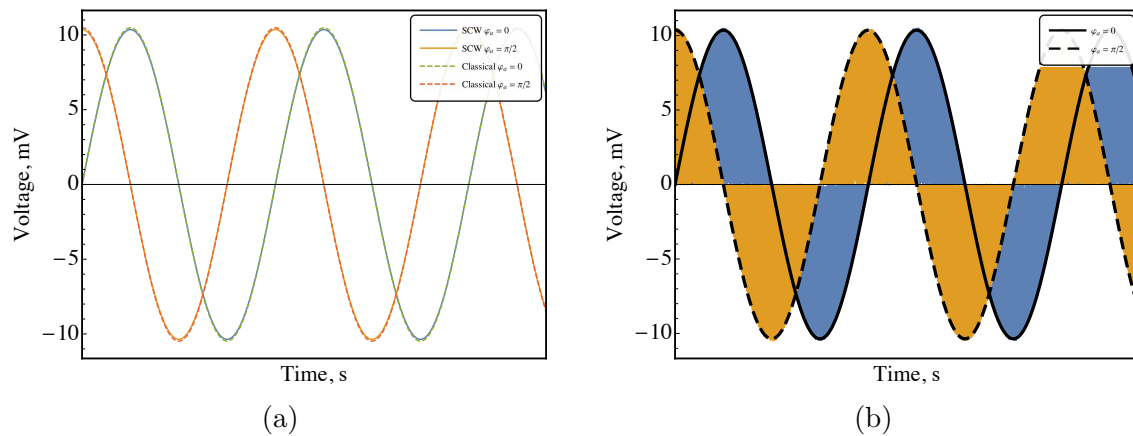


Figure 9: The detectable signal, depending on time, a corresponding phase shift will be observed. In (a) coincidence of classical heterodyne scheme and SCW analog proposed in this paper can be obtained. A result modulated signal with many sidebands is depicted in (b). Next, one can use the common phase detection methods.

of frequency Ω leads to difficulty in spectral filtering. However, we are able to experimentally demonstrate the possibility to obtain the intermediate frequency by applying photodetector with 6.17 GHz bandwidth to the single arm of the scheme Fig. 8. As one can see from the Fig. 10 the signal light is down-converted to the intermediate frequency which coincides with the microwave field frequency of electro-optical phase modulator.

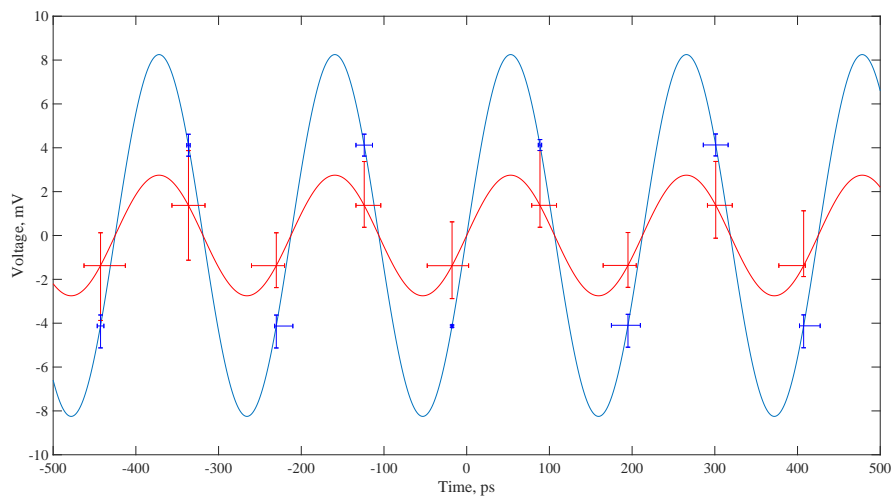


Figure 10: The dependence of output voltage on the time from the single arm of the scheme proposed ($P_c = 225.00 \mu\text{W}$, $P_s = 146.50 \mu\text{W}$) and a voltage of the microwave field of the electro-optical phase modulator.

6. Conclusion

We have demonstrated various models of coherent detection in the framework of the SCW method. All models were considered in terms of wave optics in order to make the analogy drawn with classical coherent detection schemes more clear. The experimental parameters were selected accordingly. Future work will be aimed at a detailed description of these detection approaches in the context of quantum optics, which will allow their legitimate employment in quantum computing in quantum cryptography, quantum calculations, and quantum tomography.

Acknowledgments

This work was financially supported by Russian Ministry of Education (Grant No. 2020-0903).

References

- [1] Anderson L I 1994 *Nicola Tesla: Lecture Before the New York Academy of Sciences - April 6, 1897* (Twenty First Century Books)
- [2] Roger B and Georges H 1952 Double heterodyne radio receiver US Patent 2,606,285
- [3] Protopopov V V 2009 *Laser Heterodyning* (Springer Berlin Heidelberg)
- [4] Ly-Gagnon D S, Tsukamoto S, Katoh K and Kikuchi K 2006 *Journal of lightwave technology* **24** 12
- [5] Tanosaki S, Sasaki Y, Takagi M, Ishikawa A, Inage H, Emori R, Suzuki J, Yuasa T, Taniguchi H, Devaraj B *et al.* 2003 *Optical review* **10** 447–451
- [6] Kikuchi K 2015 *Journal of Lightwave Technology* **34** 157–179
- [7] Mecozzi A and Shtaif M 2018 *Optics express* **26** 33970–33981
- [8] Lu Y, Zhu T, Chen L and Bao X 2010 *Journal of lightwave Technology* **28** 3243–3249
- [9] Yuen H P and Chan V W 1983 *Optics letters* **8** 177–179
- [10] Barchielli A 1990 *Quantum Optics: Journal of the European Optical Society Part B* **2** 423
- [11] Wallentowitz S and Vogel W 1996 *Physical Review A* **53** 4528
- [12] Grosshans F, Van Assche G, Wenger J, Brouri R, Cerf N J and Grangier P 2003 *Nature* **421** 238–241
- [13] Hirano T, Yamanaka H, Ashikaga M, Konishi T and Namiki R 2003 *Physical Review A* **68** 042331
- [14] Leverrier A and Grangier P 2011 *Physical Review A* **83** 042312
- [15] Heid M and Lütkenhaus N 2006 *Physical Review A* **73** 052316
- [16] Brádler K and Weedbrook C 2018 *Physical Review A* **97** 022310
- [17] Papanastasiou P, Lupo C, Weedbrook C and Pirandola S 2018 *Physical Review A* **98** 012340
- [18] Ghorai S, Grangier P, Diamanti E and Leverrier A 2019 *Physical Review X* **9** 021059
- [19] Merolla J M, Mazurenko Y, Goedgebuer J P, Porte H and Rhodes W T 1999 *Optics letters* **24** 104–106
- [20] Mora J, Ruiz-Alba A, Amaya W, Martínez A, García-Muñoz V, Calvo D and Capmany J 2012 *Optics letters* **37** 2031–2033
- [21] Gleim A, Egorov V, Nazarov Y V, Smirnov S, Chistyakov V, Bannik O, Anisimov A, Kynev S, Ivanova A, Collins R *et al.* 2016 *Optics express* **24** 2619–2633
- [22] Miroshnichenko G, Kozubov A, Gaidash A, Gleim A and Horoshko D 2018 *Optics express* **26** 11292–11308
- [23] Gaidash A, Kozubov A and Miroshnichenko G 2019 *JOSA B* **36** B16–B19

- [24] Chistiakov V, Kozubov A, Gaidash A, Gleim A and Miroshnichenko G 2019 *Optics Express* **27** 36551–36561
- [25] Kynev S M, Chistyakov V V, Smirnov S V, Volkova K P, Egorov V I and Gleim A V 2017 *Journal of Physics: Conference Series* **917** 052003
- [26] Samsonov E, Goncharov R, Gaidash A, Kozubov A, Egorov V and Gleim A 2020 *Scientific Reports* **10** 10034
- [27] Fang J, Huang P and Zeng G 2014 *Physical Review A* **89** 022315
- [28] Gyongyosi L and Imre S 2019 *Journal of Statistical Physics* **177** 960–983
- [29] Wang Y, Mao Y, Huang W, Huang D and Guo Y 2019 *Optics express* **27** 25314–25329
- [30] Haykin S 2008 *Communication systems* (John Wiley & Sons)
- [31] Miroshnichenko G P, Kiselev A D, Trifanov A I and Gleim A V 2017 *JOSA B* **34** 1177–1190
- [32] Capmany J and Fernández-Pousa C R 2010 *JOSA B* **27** A119–A129
- [33] Kumar P and Prabhakar A 2008 *IEEE journal of quantum electronics* **45** 149–156
- [34] Yariv A and Yeh P 1984 *Optical waves in crystals* vol 5 (Wiley New York)
- [35] Gonzalez N G, Zibar D, Yu X and Monroy I T 2010 Optical phase-modulated radio-over-fiber links with k-means algorithm for digital demodulation of 8psk subcarrier multiplexed signals *Optical Fiber Communication Conference* (Optical Society of America) p OML3
- [36] Gasulla I and Capmany J 2012 *Optics express* **20** 11710–11717
- [37] Zhang Y, Xu K, Zhu R, Li J, Wu J, Hong X and Lin J 2008 *Optics letters* **33** 2332–2334
- [38] Hirano T, Ichikawa T, Matsubara T, Ono M, Oguri Y, Namiki R, Kasai K, Matsumoto R and Tsurumaru T 2017 *Quantum Science and Technology* **2** 024010
- [39] Leverrier A 2009 *Theoretical study of continuous-variable quantum key distribution* Ph.D. thesis Télécom ParisTech
- [40] Gebbie H, Stone N, Putley E and Shaw N 1967 *Nature* **214** 165–166
- [41] Maznev A, Nelson K and Rogers J A 1998 *Optics letters* **23** 1319–1321
- [42] Fried D L 1967 *Proceedings of the IEEE* **55** 57–77
- [43] DeLange O 1968 *IEEE spectrum* **5** 77–85
- [44] Bylina M, Glagolev S and Diubov A 2017 *Proceedings of Telecommunication Universities* **3** 21–28
- [45] Wang C, Qu Y and Tang Y P T 2015 *Infrared Physics & Technology* **72** 191–194
- [46] Bohme R and Eichin M 1999 Heterodyne receiver with synchronous demodulation for receiving time signals US Patent 5,930,697
- [47] Chen Y K, Koc U V and Leven A 2010 Optical heterodyne receiver and method of extracting data from a phase-modulated input optical signal US Patent 7,650,084

This figure "graph.png" is available in "png" format from:

<http://arxiv.org/ps/2006.16543v1>